Crystallization Kinetics as a Probe of the Dynamic Network in Lightly Sulfonated Syndiotactic Polystyrene Ionomers

E. Bruce Orler, Bret H. Calhoun, and Robert B. Moore*

Department of Polymer Science, University of Southern Mississippi, P.O. Box 10076, Hattiesburg, Mississippi 39406-0076

Received January 2, 1996; Revised Manuscript Received June 3, 1996[⊗]

ABSTRACT: The effect of alkali metal counterion type on the crystallization kinetics of sulfonated syndiotactic polystyrene with ion contents of 1.4 mol % was investigated. For crystallization temperatures less than 180 °C, the rate of crystallization was independent of counterion type. In contrast, for temperatures greater than 180 °C, the rate of crystallization increased with increasing counterion size. Since the glass transition and melting temperatures were found to be constant for all counterion types, the variations in crystallization behavior were attributed to differences in chain diffusion within the dynamic network of electrostatic cross-links. At low temperatures, the rate of ion-hopping is slow for all of the counterion forms relative to the rate of crystallization, and thus crystal growth occurred in the presence of kinetically stable cross-links. At high temperatures, chain diffusion is controlled by the ion-hopping process, and the kinetics of crystallization become influenced by the strengths of ionic interactions. Between 180 and 215 °C, the rate of crystallization was found to be inversely proportional to the ionic radii of the counterions. As the activation energy for ion-hopping increased with decreasing counterion size, longer periods of time were required to achieve the same degree of crystallinity.

Introduction

The random incorporation of small quantities of noncrystallizable comonomer units into the backbone of a semicrystalline polymer has a dramatic effect on the thermodynamics and kinetics of crystallization.[1−6] Relative to the behavior observed with homopolymers, crystallizable copolymers usually exhibit lower melting temperatures, lower degrees of crystallinity, and a significant decrease in the overall rate of crystallization. In many systems, this behavior has been attributed to an exclusion of noncrystallizable units from the crystalline lamella.[1,4,5] As the concentration of noncrystallizable units in the copolymer increases, the average length and volume fraction of crystallizable segments decreases. Furthermore, as these copolymers crystallize, the excluded units become concentrated in the melt, which consequently retards the rate of crystallization.

The incorporation of cross-linked units into a semicrystalline polymer has also been shown to affect the thermodynamics and kinetics of crystallization.[1,7−9] In a manner similar to that observed with the semicrystalline copolymers, cross-linked units in polymer networks are also excluded from the crystallites.[1] However, it is important to note that copolymers contain units which limit longitudinal crystal growth while covalent cross-links can limit both longitudinal and lateral growth. The effect of intermolecular cross-linking on crystallization has been demonstrated by comparing the observed melting point depressions of unoriented polymer networks to those predicted for analogous random copolymers containing similar mole fractions of noncrystallizable units. For a given quantity of noncrystallizable units, the melting point depressions in randomly cross-linked materials are substantially lower than those predicted for random copolymers.[1] In addition, the degree of crystallinity and rate of crystallization have been observed to decrease with increasing levels of cross-linking.[9]

With respect to the crystallization kinetics of polymers containing noncrystallizable units, a fundamental difference between network systems and random copolymers stems from the relative effects that the noncrystallizable units have on chain mobility. The covalent cross-links in network systems permanently restrict interchain mobility. In contrast, the noncrystallizable units in copolymers generally act as random, noninteracting defects which do not affect interchain mobility. As an intermediate system, semicrystalline ionomers are random copolymers which contain noncrystallizable, *interactive* groups capable of forming thermally labile, electrostatic cross-links.[10−13] In the melt state, these Coulombic associations form a *dynamic* network in which the ion pairs can transfer between aggregates via a kinetic ion-hopping process.[10] Thus, depending on the strength of interactions between the ionic groups, noncrystallizable units in semicrystalline ionomers may affect crystallization in a manner which varies between the "extreme" effects observed in random copolymers and covalently cross-linked systems.

We have recently initiated studies aimed at understanding the link between ionic aggregation and crystallization in lightly sulfonated syndiotactic polystyrene (SsPS) ionomers.[14−16] Since a wealth of experimental and theoretical information on ionic aggregation exists for sulfonated atactic polystyrene (SaPS) ionomers,[17−26] sulfonated syndiotactic polystyrene is an optimal choice for these fundamental investigations. By comparing the structure−property relationships of SaPS to that of the new SsPS ionomers, the role of electrostatic interactions on crystallization can be determined. Moreover, the crystallization behavior of SsPS provides a unique probe for monitoring the strength of electrostatic interactions between the noncrystallizable ionic units.

Experimental Section

Materials. The syndiotactic polystyrene with greater than 99% purity had a weight-average molecular weight of 609 000 g/mol and was obtained from Dow Chemical Co. Diethyl ether and 1,1,2-trichloroethane were obtained from Fisher; all other chemicals were obtained from Aldrich and used without further purification.

Preparation of the Sulfonating Reagent. Concentrated sulfuric acid (0.018 mol) was slowly added, with vigorous

* Author to whom all correspondence should be addressed.
[⊗] Abstract published in *Advance ACS Abstracts,* August 1, 1996.

S0024-9297(96)00003-4 CCC: $12.00

stirring, to 25 mL of a 1,1,2-trichloroethane solution containing 0.03 mol of caproic anhydride. After complete mixing, the concentrated reagent was equilibrated at room temperature and then diluted with 1,1,2-trichloroethane to 50 mL in a volumetric flask.

Sulfonation of Syndiotactic Polystyrene. In a 1000-mL round-bottom flask, 10.0 g of syndiotactic polystyrene (sPS) was mixed with 700 mL of 1,1,2-trichloroethane and heated under reflux (ca. 115 °C) until all the sPS dissolved. The solution was then transferred to a hot water bath and equilibrated to 60 °C. With rapid stirring, 6.4 mL of the caproic anhydride sulfonating reagent in 1,1,2-trichloroethane was slowly added to the sPS solution. The reaction was allowed to proceed for 1 h at 60 °C and then terminated by the addition of 20 mL of methanol. To avoid gelation after the reaction was terminated, the warm solution was immediately precipitated into 1500 mL of cold diethyl ether. The precipitate was then filtered and dried under a nitrogen purge overnight.

Due to rapid solvent-induced crystallization of syndiotactic polystyrene, a Parr pressure reactor was used to dissolve the polymer in a 95:5 (v/v) mixed solvent of chloroform and methanol at elevated temperatures (i.e., 100 °C). Once cooled to room temperature, these dilute SsPS solutions were found to be homogeneous (i.e., no observable crystallization) for several hours. To facilitate the complete removal of residual sulfonating reagent from the functionalized polymer, the sulfonated syndiotactic polystyrene (SsPS) samples, dissolved in chloroform/methanol, were steam stripped into boiling deionized (DI) water. The precipitate was then ground into a fine slurry in methanol using a Waring blender. Finally, the polymer was filtered and dried in a vacuum oven, at 70 °C, overnight. To determine the mole percent sulfonation, 0.3−0.5 g samples of the SsPS were dissolved in 100 mL of chloroform/methanol and then titrated to the phenolphthalein end point using standardized methanolic NaOH.

Neutralization. Solutions containing 0.4 g of SsPS were dissolved in a 95:5 (v/v) mixed solvent of chloroform and methanol as described above. For each of the counterion forms used in this study, SsPS solutions were neutralized by adding a quantitative amount of methanolic NaOH, KOH, RbOH, or CsOH titrant. After stirring under a N_2 purge for 60 min, these samples were then steam stripped in boiling DI water. The neutralized precipitates were collected and then dried in a vacuum oven at 80 °C for 48 h.

Optical Microscopy. Equilibrium melting temperatures of the SsPS ionomers were evaluated using a Mettler FP82HT hot stage mounted on a Nikon Optiphot2 polarizing optical microscope. Thin samples of the ionomers were heated, in a nitrogen atmosphere, to 330 °C, held for 3 min, and then cooled at ca. −20 °C/min to the isothermal crystallization temperature. After the samples had crystallized, the temperature was jumped to 250 °C followed by a slow heating ramp of 1 °C/min. The optical melting point was chosen as the temperature at which all birefringence had disappeared. The equilibrium melting temperatures, $T_m°$, of sPS and the SsPS ionomers were then determined by plotting the optical melting points versus crystallization temperature; the point of intersection between the theoretical line defined by $T_m = T_c$ and the extrapolated experimental data yields the equilibrium melting temperature.

Thermal Analysis. The thermal properties and crystallization kinetics of the SsPS ionomers were compared using a Perkin-Elmer DSC 7 differential scanning calorimeter, with a nitrogen purge. The glass transition temperatures, T_g's, were determined as the midpoint of the step change in the heat flow. The melting, T_m, and crystallization, T_c, temperatures were selected as the peak maximum or minimum in endothermic or exothermic transitions, respectively.

For the isothermal crystallization studies, all samples were initially heated to 330 °C for a period of 3 min to normalize the thermal history. These samples were then quenched at a cooling rate of −200 °C/min to the isothermal crystallization temperatures, and the crystallization exotherm was monitored as a function of time. The half-time, $t_{1/2}$, of crystallization (i.e., the time required for the material to reach 50% of its maximum crystallinity) was used as a quantitative comparison

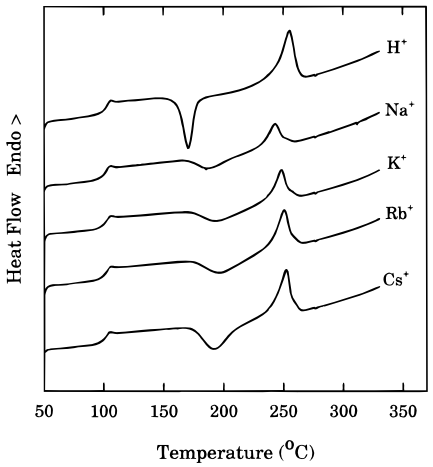

Figure 1. Effect of alkali metal counterion type on the thermal behavior of melt-quenched SsPS ionomers containing ion contents of 1.4 mol %. All thermograms are normalized with respect to sample mass and were acquired during a heating scan of 20 °C/min.

of the rate of bulk crystallization with changes in counterion type and crystallization temperature. The isothermal crystallization data were analyzed using the Avrami equation,[27]

$$\ln[-\ln(1 - X_c(t))] = \ln K + n \ln t \tag{1}$$

where K is the kinetic growth rate constant, n is the Avrami exponent, and $X_c(t)$ is the relative extent of crystallization at time t. From the DSC data, $X_c(t)$ is defined as

$$X_c(t) = \frac{\int_0^t \left(\frac{dH}{dt}\right) dt}{\int_0^\infty \left(\frac{dH}{dt}\right) dt} \tag{2}$$

where (dH/dt) is the rate of heat evolution during crystallization as a function of time.

Dynamic Mechanical Analysis. Dynamic mechanical measurements using a Seiko Instruments SDM 5600 Series dynamic mechanical spectrometer were performed on thin bars of sulfonated atactic polystyrene ionomers. All samples were compression molded at 180 °C, and the sample cross-sectional areas were ca. 8 mm^2. The samples were analyzed in the tensile mode using the DMS 210 module at a deformation frequency of 1 Hz and a strain amplitude of 6.5 μm.

Results

Thermal Properties of SsPS. Figure 1 shows the effect that various alkali metal counterions have on the thermal behavior of melt-quenched, sulfonated syndiotactic polystyrene ionomers containing ion contents of 1.4 mol %. The DSC heating scans of the melt-quenched ionomers show similar thermal behavior for all the alkali metal counterions (i.e., glass transition, crystallization exotherm, and a melting endotherm). For these low ion contents, neutralization and/or counterion type has little effect on the T_g of SsPS. In contrast, the various counterions have significant effects on the crystallization and melting behavior of these materials.

The crystallization exotherm of the acid form SsPS (Figure 1) occurs at the lowest temperature and has the sharpest crystallization exotherm. Neutralization of this SsPS with alkali metal counterions increases the temperature required for crystallization and broadens the crystallization peak. For the series of neutralized ionomers, the crystallization exotherms sharpen and the melting endotherms increase in magnitude with increasing counterion size. A comparison of the heat of

Table 1

sample	T_m* (°C)[a]
pure sPS	275
1.4 mol % H^+-form SsPS	
predicted[b]	270
observed	270
1.4 mol % SsPS ionomers	
Na^+-form	267
K^+-form	268
Rb^+-form	268
Cs^+-form	268

[a] Extrapolated melting temperature, determined by extrapolating plots of the optical melting points vs crystallization temperature to the theoretical line defined by $T_m = T_c$.[28] [b] Melting point depression as predicted using Flory's copolymer relationship.[33]

crystallization, ΔH_c, to the heat of melting, ΔH_f, indicates (within experimental error) that all of these ionomers crystallize predominantly during the heating rescan. In addition to changes in the magnitude of the melting endotherm, these data show that the peak melting temperature increases with counterion size from 243 (Na^+-form) to 252 °C (Cs^+-form). Note that the peak melting temperature for the Cs^+-form SsPS is comparable to that of the acid-form SsPS (254 °C).

Table 1 summarizes the melting point data for sPS and SsPS ionomers with an ion content of 1.4 mol %. In contrast to the dynamic melting points observed in the DSC data of Figure 1, the melting temperatures in Table 1 were obtained from *isothermally* crystallized samples. Using the Hoffman−Weeks approach,[28] plots of the observed T_m versus the isothermal crystallization temperature, T_c, were extrapolated to the theoretical $T_m = T_c$ line in order to obtain an estimate of the "equilibrium" melting temperature. The extrapolated melting temperature for sPS was found to be 275 °C; this value is in excellent agreement with previous reports of the equilibrium melting temperature for sPS.[29−32]

Since the concept of infinitely thick crystallites is invalid for copolymers,[3] it is important to note that the extrapolated melting temperatures, T_m*, for the SsPS materials are not to be considered as equilibrium melting points. Nevertheless, these data do serve as a means of systematically comparing the effects of sulfonation and neutralization on the melting behavior of SsPS ionomers with identical thermal histories. For the acid-form SsPS sample, the *extrapolated* melting temperature was determined to be 270 °C. After neutralization with alkali metal counterions, the extrapolated melting temperatures of the 1.4 mol % SsPS ionomers were determined to be ca. 268 °C and independent of counterion type. In contrast to the melting point depression observed in the nonequilibrium DSC data of Figure 1, the counterion type has little (if any) effect on the extrapolated T_m for the ionomers containing 1.4 mol % ionic groups.

For the isothermally crystallized samples, the melting point depressions in Table 1 were compared with the theoretical predictions of melting point depression in a random, crystallizable copolymer containing noncrystallizable monomer units. Flory proposed that melting point depression by random incorporation of noncrystallizable monomer units into a crystallizable backbone may be calculated following the relationship:[33]

$$\frac{1}{T_m^*} - \frac{1}{T_m^\circ} = -\frac{R}{\Delta H_u} \ln n \qquad (3)$$

where T_m° is the equilibrium melting point of the analogous homopolymer (i.e., sPS), T_m* is the extrapolated melting point of the copolymer (i.e., SsPS), R is the gas constant, ΔH_u is the heat of fusion per mole of crystallizable units, and n is the mole fraction of crystallizable units. Pasztor and co-workers determined the ΔH_u for pure sPS to be 5.58 kJ/mol.[34]

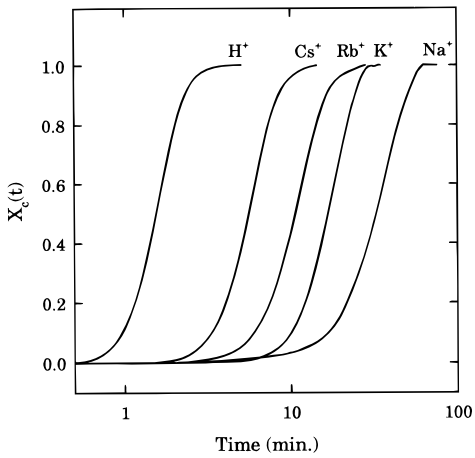

Figure 2. Effect of alkali metal counterion type on the isothermal crystallization of SsPS containing ion contents of 1.4 mol % at T_c = 210 °C.

Using Flory's copolymer analysis,[33] the melting point depression for a copolymer of sPS containing 1.4 mol % of noncrystallizable monomer units is predicted to be 5 deg. For the H^+-form SsPS containing 1.4 mol % sulfonated styrene units, the experimentally observed melting point depression is 5 deg. Although the theoretically predicted melting point depression is dependent on the choice of an experimentally determined ΔH_u, the calculated and observed melting point depressions are in excellent agreement. Therefore, these data indicate that the bulky sulfonic acid units are not incorporated into the sPS crystalline lattice and reside only in the amorphous phase.[15,35]

Once the H^+-form SsPS has been neutralized, the T_m is depressed by an additional 2−3 deg. This behavior has also been observed with ethylene-based ionomers[36] and demonstrates that the ionic groups are also excluded from the crystalline domains and inhibit crystal growth along the polymer chain direction (i.e., obstruct lamellar thickening) to an extent greater than that expected from the simple noncrystallizable-comonomer exclusion effect.[33] Future investigations of SsPS ionomers of different ion contents will be aimed at developing a precise explanation for the influence of ionic aggregation on the melting point depression in semicrystalline ionomers.

Isothermal Crystallization Kinetics of SsPS. Figure 2 shows the effect of counterion type on the crystallization profiles of SsPS ionomers that were isothermally crystallized at 210 °C. Each of the isotherms display the characteristic sigmoidal shape, which is typical of a nucleation and growth crystallization process. Since these polymers have the same mole fraction of functionalized units and identical sequence length distributions of crystallizable segments, it is clear that the type of counterion has a strong influence on the rate of crystallization. The rate of overall crystallization for the H^+-form sample is significantly faster than for the neutralized ionomers. However, within the set of neutralized SsPS materials, the time required for crystallization increases with decreasing counterion size.

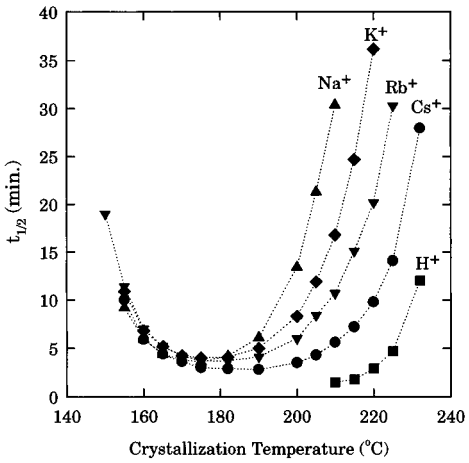

Figure 3. Effect of isothermal crystallization temperature on the half-time of crystallization for 1.4 mol % SsPS ionomers neutralized with various counterions.

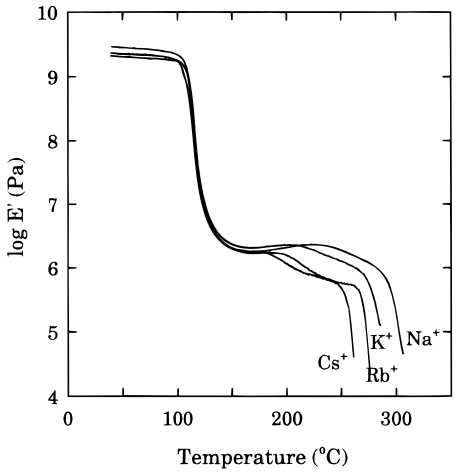

Figure 4. Effect of alkali metal counterion type on the dynamic mechanical properties of sulfonated atactic polystyrene ionomers containing 2.1 mol % ionic groups.

While the rates of SsPS crystallization are influenced by counterion type, the qualitative shape of the isotherms in Figure 2 does not vary with counterion and the isotherms are reasonably superimposable. When these data were analyzed using the Avrami approach[27] (as per eq 1), the Avrami exponents, n, for the ionomers were determined to be in the range 2.8−3.3 (the linear regression correlation coefficients were at least $r^2 = 0.999$). In addition, the Avrami rate constants, K, were found to decrease from 2×10^{-3} min^{-1} for the Cs^+ sample to 5×10^{-5} min^{-1} for the Na^+ sample. Therefore, these data suggest that while the rate of crystallization is strongly affected by counterion size, the principal mechanism for crystallization of SsPS is not a function of counterion type.

Figure 3 shows the temperature dependence on the bulk crystallization rates (as measured by crystallization half-times, $t_{1/2}$) of SsPS ionomers with ion contents of 1.4 mol %. Note that $t_{1/2}$ is inversely related to the overall rate of crystallization such that the higher the $t_{1/2}$, the slower the rate of crystallization. For a given counterion type (e.g., Cs^+-form SsPS), the shape of the $t_{1/2}$ versus temperature curve is characteristic of typical semicrystalline polymers. The rate of transport of chain segments to the crystallite surface competes with the rate of nucleation and consequently, the $t_{1/2}$ displays a minimum between the extremes of T_g and T_m.

For isothermal crystallization temperatures above 180 °C, the rate of crystallization becomes dependent on counterion type such that $t_{1/2}$ decreases with an increase in the size of the counterion. Moreover, as the crystallization temperature increases, differences between the $t_{1/2}$ values for the various counterions become greater. As an exception to this trend, it is important to note that the rates of crystallization observed for the H^+-form SsPS are faster than those observed for the neutralized ionomers.

In contrast to the influence of counterion type at high temperatures, isothermal crystallization of SsPS below 180 °C yields $t_{1/2}$ values that are independent of counterion type. The $t_{1/2}$ versus T_c curves for all of the counterions are superimposable and simply increase with decreasing temperature (i.e., diffusion-controlled behavior). Note that due to the time required to cool from the melt and stabilize the DSC at the isothermal crystallization temperature, kinetic data for the rapidly crystallizing H^+-form SsPS were not obtained in this temperature range.

Dynamic Mechanical Properties of SaPS. Since SsPS ionomers containing less than 2 mol % ionic groups crystallize, sulfonated atactic polystyrene ionomers were utilized to "model" the influence of counterion type on the viscoelastic properties of the amorphous (melt) state. Figure 4 shows the effect of alkali metal counterion type on the dynamic mechanical properties of SaPS ionomers containing ion contents of 2.1 mol %. For temperatures less 180 °C, the storage modulus vs temperature curves are independent of counterion type. However, for temperatures greater than 180 °C, the counterion type has a significant effect on the dynamic mechanical response. The length of the rubbery plateau region and the temperature at which flow begins increase with decreasing counterion size. Similar results have been reported by Hara et al. for the viscoelastic properties of sulfonated atactic polystyrene with ion contents of 4.1 mol %.[37]

Discussion

Previous studies have demonstrated that the thermal, mechanical, and rheological properties of atactic polystyrene-based ionomers can be influenced by changing the type of ionic groups incorporated onto the polymer chains.[10,13,17,26] In general, these variations in properties with ion type have been attributed to distinct differences in the strengths of electrostatic interactions between the ion pairs. For a given ionomer, the type of counterion may be used to alter the Coulombic interactions between ion pairs and thus to control the strength of the electrostatic cross-links. Since the ion pairs in ionomers act as permanent dipoles, the energy of interaction between two dipoles may be obtained by applying Coulomb's law to the four elements of charge.[38] For two dipoles A and B separated by a distance d, the energy of the dipole−dipole interaction, ϕ_{dd}, is a function of their respective dipole moments, μ_i, separation distance, and relative orientations as given by

$$\phi_{dd} = -\frac{\mu_A \mu_B}{d^3}[2 \cos \theta_A \cos \theta_B - \sin \theta_A \sin \theta_B \cos(\psi_A - \psi_B)] \quad (4)$$

where θ_A and θ_B are the angles of inclination of the polar axes to the line of centers, and ψ_A and ψ_B are the angles subtended between the polar axes and perpendiculars

passing through their centers. Thus, for an ionomer of a given counterion type, the attractive energy between dipoles in head-to-tail orientations is proportional to μ^2 and inversely proportional to d^3.

For the series of ionomers studied here, the anion type is fixed while the cation type is varied within the group of alkali metal ions. In considering the influence of counterion type on the dipole−dipole interactions, it is important to note that the cation size affects both the dipole moment and the minimum separation distance. While the dipole moment increases with charge separation, such that μ_{Cs} is greater than μ_{Na}, the electronic polarizabilities of the alkali metal ions have been found to increase by over an order of magnitude in the order $Na^+ < K^+ < Rb^+ < Cs^+$.[39] This trend in polarizability counteracts the effect of charge separation and tends to diminish the relative differences between the dipole moments of ion pairs containing the alkali metal ions. Note that while this argument maintains a larger dipole moment for $SO_3^-Cs^+$ groups in comparison to that of the $SO_3^-Na^+$ groups, the relative differences in μ_i (within the series of alkali metal ions) are less than that predicted by treating the ions as simple point charges.

As the ion pairs pack into multiplets, it is reasonable to expect that the size of the counterion would affect the packing efficiency (or density) and the minimum dipole−dipole separation distance. Since the Na^+ ions are much smaller than the Cs^+ ions, the average d between $SO_3^-Na^+$ groups is expected to be smaller than that for the larger $SO_3^-Cs^+$ groups. Therefore, since the overall dipole−dipole interaction energy decreases with the third power d and increases with the second power μ, the above arguments suggest that ϕ_{dd} should tend to decrease with increasing counterion size.

In agreement with previous studies of SaPS ionomers, the results of this study indicate that the choice of ion type may also be used to control the physical properties of SsPS ionomers. While the T_g's for the SsPS (Figure 1) and SaPS ionomers (Figure 4) are insensitive to changes in counterion type at these relatively low ion contents, the influence of ion type in SsPS is most evident in the systematic changes in properties associated with the crystalline state. The DSC data of the melt-quenched SsPS ionomers (Figure 1) indicate that the counterion type affects the ability of these materials to crystallize. Furthermore, the shift to lower temperatures of the dynamic T_m and the observed decrease in ΔH_f with decreasing counterion size yield indirect evidence that the crystallization kinetics of these polymers are influenced by the strength of electrostatic interactions.

Direct evidence for the link between crystallization kinetics and the strength of electrostatic cross-links is obtained from the data in Figure 2. As the size of the counterion decreases, the dipole−dipole interactions between ion pairs become stronger which increases the stability of the physically cross-linked network. Consequently, chain diffusion and mobility of the crystallizable segments diminishes, and thus the crystallization process is slowed. Note that these kinetic data result from the observation of *bulk* crystallization; future spherulitic growth rate studies of these ionomers will be aimed at separating the effects of ionic interactions on nucleation from the effects on crystal growth.

In contrast to the trend observed with counterion size in the neutralized samples, the H^+-form SsPS sample in Figure 2 displays the fastest rate of crystallization. This behavior may also be attributed to the relative strengths of interactions between the functional groups. The sulfonic acid groups yield weak hydrogen-bonding interactions relative to the strong Coulombic interactions between the neutralized sulfonate groups. With weak interactions, chain diffusion is high and thus the rate of crystallization is fast.

The temperature dependence of the crystallization half-time (Figure 3) indicates that the crystallization kinetics of SsPS are affected by the strength of electrostatic interactions only at high temperatures. For temperatures below 180 °C, the crystallization curves are superimposible. Based on the DSC data in Figure 1 and the melting point data in Table 1, it is important to note that T_g and T_m are identical for each of the counterion types. Furthermore, the temperature of maximum crystallization rate (i.e., minimum $t_{1/2}$) is constant at ca. 180 °C for all of the ionomers shown in Figure 3. Thus, the observed shifts in crystallization rate at temperatures above 180 °C are not due to a limitation in the crystallization window (i.e., the range between T_g and T_m) or to a change in the degree of supercooling at a given T_c.

The distinct difference between the crystallization behavior above and below 180 °C may be understood by considering the balance between elastic and electrostatic forces in ionomers. The elastic force, f, acting on a polymer chain segment between ion pairs (located in different aggregates) may be given by[11]

$$f = 3kTr/\bar{r}^2 \tag{5}$$

where $\bar{r}^2$ is the mean square end-to-end distance of the free chain segment, r is the actual separation of the two ion pairs, and kT is the thermal energy. This elastic force increases with temperature and tends to oppose the electrostatic forces which cause the ions to aggregate. Note that with respect to Coulomb's law (see eq 4), the electrostatic forces are assumed to be independent of temperature.[11] As the temperature increases, the elastic forces rise to counterbalance the electrostatic forces. Consequently, the ionic aggregates become kinetically unstable[10] such that ion pairs can be pulled out of the aggregates in order to relieve local stress.

The phenomenon of an ion pair transferring from one aggregate to another in order to satisfy the local balance between elastic and electrostatic forces is referred to as ion hopping and defines the dynamic network in ionomers.[10,13,40] This thermally activated process is responsible for ionomer flow and melt processability at elevated temperatures. During an ion-hopping event, polymer chain segments adjacent to the migrating ion pair experience an increase in mobility. As the frequency of ion-hopping events increases, a significant quantity of chains become mobilized, and the bulk viscoelastic behavior of the polymer adopts a more liquid-like character. In the general case of semicrystalline ionomers, the ability of the material to crystallize is a function of chain mobility/diffusion and thus directly linked to the process of ion hopping.

Leibler et al. have studied the dynamics of reversible networks and found that the mobility of polymer chains in hydrogen-bonding systems is controlled by the concentration and lifetime of the temporary cross-links.[41] On time scales of these lifetimes, the "stickers" can break away from one tie point and reassociate at another tie point. Thus, chains can diffuse in reversible

networks, and stress can relax. This treatment describes, in general, the process of ion hopping in ionomers. However, since ion pairs can associate into multiplets of various sizes and shapes,[12,41] the consideration of ionomer dynamics is complex and proposed to rely on a distribution of microscopic junction lifetimes.[41] In agreement with this model, it is reasonable to conclude that the lifetime of an ion pair in an electrostatic cross-link, and thus the kinetics of ion hopping, is governed by the balance between elastic and electrostatic forces. At a given temperature above T_g, the cross-link lifetimes are expected to increase with an increase in electrostatic attractive forces. Therefore, the rate of ion hopping and ionomer chain diffusion decrease with an increase in the strength of dipole−dipole interactions between associating ion pairs.

The kinetic data in Figure 3 reflect the influence of ion-hopping kinetics on the rate of crystallization. For temperatures below 180 °C, the elastic forces are weaker than the electrostatic forces, and the rate of ion hopping is slow. Thus, on the time scale of the crystallization process, all of the ionomers contain kinetically stable multiplets that act as irreversible cross-links, regardless of counterion type.

As the temperature increases above 180 °C, each of the samples in Figure 3 shows an expected decrease in crystallization rate. This temperature regime is classically referred to as the interfacially controlled region; however, it is important to note that the contribution from chain diffusion at these temperatures can still influence the overall rate of crystallization. For temperatures greater than 180 °C, the elastic forces are comparable to the electrostatic forces, and the rate of ion hopping is fast. At these temperatures, the rates of ion hopping and crystallization are on the same time scale and kinetically coupled by their respective effect and dependence on chain diffusion. As the counterion size increases, the diffusion of crystallizable chain segments is facilitated, and the ionomer crystallizes in a shorter period of time. Since this coupling or link between ion hopping and crystallization mechanisms is only observed at relatively high temperatures, it is not surprising that the crystallization of polyethylene-based ionomers (which melt below ca. 120 °C) has been found to be insensitive to counterion type.[42]

The above argument attributes the high-temperature crystallization behavior observed in Figure 3 to the effects of ionic interactions on chain diffusion. If, on the other hand, the strength of ionic interactions significantly influenced the nucleation behavior, then the high-temperature data in Figure 3 would suggest that the nucleation half-time for the Cs^+-form SsPS would be less than that of the Na^+-form SsPS. However, since ionic aggregates have been shown to restrict the mobility of chain segments,[12,43] the local *mobility* of the crystallizable segments between the ionic units would be expected to decrease with *decreasing* counterion size. This reduction in segmental mobility would consequently lead to a decrease in nucleation half-time with decreasing counterion size. Thus, if ionic interactions significantly influenced the nucleation half-time, then the effect of counterion size would yield a trend opposite to that observed in Figure 3. Therefore, based on these arguments, the data in Figure 3 strongly suggest that the effects of counterion type on the crystallization kinetics of SsPS originate predominantly from differences in chain diffusion.

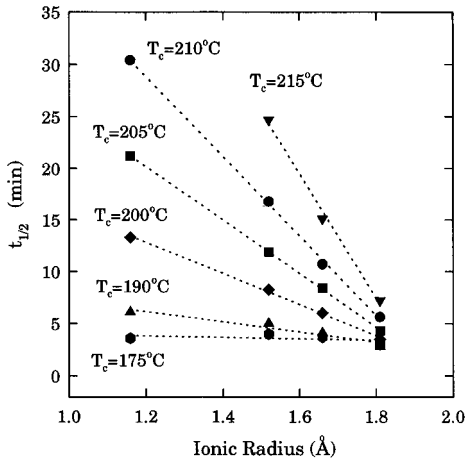

Figure 5. Correlation of crystallization half-time with the ionic radii of the alkali metal counterions at various isothermal crystallization temperatures.

The link between ion hopping kinetics and crystallization kinetics is further supported by the DMA data in Figure 4. In agreement with the data in Figure 3, the rheological properties of the ionomers are virtually identical at temperatures below 180 °C, while systematic effects of counterion size are observed at higher temperatures. Of specific interest, the temperature characteristic of the onset of rubbery flow increases with decreasing counterion size. Eisenberg and co-workers[10,13] have demonstrated that the frequency dependence of this viscoelastic response may be used to evaluate the activation energies for ion hopping, E_a. Moreover, Horrion et al. have shown that activation energies for ion hopping in α,ω-dicarboxylatopolybutadiene telechelic ionomers increase linearly with a decrease in the radii of alkali cations.[44] Thus, the data in Figure 4 and the effect of counterion size on the rate of SsPS crystallization suggest that the activation energy for ion hopping in sulfonated polystyrene ionomers increases with a decrease in the counterion size.

To quantitatively compare the effects of counterion size on the crystallization kinetics, the crystallization half-time data from Figure 3 were plotted versus the ionic radii for temperatures above 180 °C (see Figure 5). These data show that the crystallization kinetics of SsPS ionomers are linearly related to the ionic radius of the counterion. As the temperature increases, the effects of counterion size become more distinct. In agreement with the viscoelastic results of Horrion et al.,[44] this increasing slope with temperature may be attributed to the different activation energies for ion hopping. For classical Arrhenius behavior, processes with higher activation energies are more temperature sensitive. Therefore, a higher E_a for ion hopping in the Na^+-form SsPS yields a greater temperature dependence in the overall rate of crystallization relative to that of the Cs^+-neutralized ionomer.

While the data in Figure 5 appear linear, it is important to note that this behavior is far from understood. In these complex systems containing noncrystallizable, interactive comonomer units, the local state of the network in the vicinity of a growing crystallite can range from a cross-linked gel to a free-flowing melt. Thus, the observation that the rate of crystallization is so simply related to ionic interactions within the amorphous component is surprising. Our future investigations of these model semicrystalline ionomers will be aimed at developing a quantitative, theoretical under-

standing of the link between ion hopping and crystallization kinetics. Furthermore, it is anticipated that this treatment will be applicable to crystallization in other dynamic networks.

Conclusions

Depending on the strength of interactions between ion pairs, the crystallization behavior of semicrystalline ionomers may range from that observed with a covalently cross-linked system to a simple copolymer containing noncrystallizable units. For random ionomers containing interactive groups, the crystallizable segments of sufficient length must organize into crystalline domains within a dynamic network. In these complex systems, simple changes in counterion type can have a significant effect on the kinetics of crystallization. However, systematic variations in crystallization behavior with counterion size and/or charge are likely to be observed only under conditions where the elastic and electrostatic forces are comparable.

For lightly sulfonated syndiotactic polystyrene containing 1.4 mol % of ionic groups, the crystallization process becomes linked to the ion hopping kinetics at elevated crystallization temperatures. At temperatures less than 180 °C, the rate of crystallization is independent of alkali metal counterion type, while at higher temperatures, the crystallization rate increases with counterion size. Since T_g and T_m were found to be the same for all counterion types, the variations in crystallization behavior are attributed to differences in chain diffusion at the specified crystallization temperature.

At low temperatures, the rate of ion hopping is slow for all of the counterion forms relative to the rate of crystallization, and thus crystal growth occurs in the presence of kinetically stable cross-links. Since the crystallization behavior for the series of neutralized ionomers is identical in the temperature range between T_g and 180 °C, it is reasonable to conclude that, at these relatively low temperatures, the effective mobility of crystallizable segments within the ionic network is similar for each of the counterion forms.

At high temperatures, however, the elastic forces which act to pull ion pairs out of multiplets increase relative to the electrostatic attractive forces. With smaller counterions (e.g., Na^+ relative to Cs^+ ions), the energy of dipole−dipole interactions is high and more thermal energy is required to activate a sufficient number of ion-hopping events for significant chain flow. Consequently, chain diffusion in the melt is controlled by the ion-hopping process, and the kinetics of crystallization become influenced by the strengths of ionic interactions. Furthermore, as the activation energy for ion hopping increases, longer periods of time are required to achieve the same degree of crystallinity.

Acknowledgment. The authors gratefully acknowledge the Mississippi NSF EPSCoR Program (Grant No. EHR-9108767) for financial support and the Dow Chemical Co. for supplying the syndiotactic polystyrene.

References and Notes

(1) Mandelkern, L. *Crystallization in Polymers*; McGraw-Hill: New York, 1964.
(2) Wunderlich, B. *Macromolecular Physics*; Academic Press: New York, 1976; Vol. 2.
(3) Alamo, R. G.; Viers, B. D.; Mandelkern, L. *Macromolecules* **1995**, *28*, 3205.
(4) Alamo, R. G.; Chan, E. K. M.; Mandelkern, L.; Voigt-Martin, I. G. *Macromolecules* **1992**, *25*, 6381.
(5) Alamo, R. G.; Mandelkern, L. *Macromolecules* **1991**, *24*, 6480.
(6) Goulet, L.; Prud'Homme, R. E. *J. Polym. Sci. Polym. Phys. Ed.* **1990**, *28*, 2329.
(7) Bekkedahl, N.; Wood, L. A. *Ind. Eng. Chem.* **1941**, *33*, 381.
(8) Mandelkern, L.; Roberts, D. E.; Halpin, J. C.; Price, F. P. *J. Am. Chem. Soc.* **1960**, *82*, 46.
(9) Gent, A. N. *J. Polym. Sci.* **1955**, *18*, 321.
(10) Hird, B.; Eisenberg, A. *Macromolecules* **1992**, *25*, 6466.
(11) Eisenberg, A. *Macromolecules* **1971**, *4*, 125.
(12) Eisenberg, A.; Hird, B.; Moore, R. B. *Macromolecules* **1990**, *23*, 4098.
(13) Kim, J. S.; Yoshikawa, K.; Eisenberg, A. *Macromolecules* **1994**, *27*, 6347.
(14) Orler, E. B.; Yontz, D. J.; Moore, R. B. *Macromolecules* **1993**, *26*, 5157.
(15) Orler, E. B.; Moore, R. B. *Macromolecules* **1994**, *27*, 4774.
(16) Orler, E. B.; Moore, R. B. *Polym. Prepr. (Am. Chem. Soc., Div. Polym. Chem.)* **1995**, *36* (2), 372.
(17) Fitzgerald, J. J.; Weiss, R. A. *J. Macromol. Sci., Rev. Macromol. Chem. Phys.* **1988**, *C28*, 99.
(18) Weiss, R. A.; Lefelar, J. A. *Polymer* **1986**, *27*, 3.
(19) Register, R. A.; Cooper, S. L. *Macromolecules* **1990**, *23*, 310.
(20) Yarusso, D. J.; Cooper, S. L. *Macromolecules* **1983**, *16*, 1871.
(21) Galambos, A. F.; Stockton, W. B.; Koberstein, J. T.; Sen, A.; Weiss, R. A.; Russell, T. P. *Macromolecules* **1987**, *20*, 3091.
(22) Register, R. A.; Sen, A.; Weiss, R. A.; Cooper, S. L. *Macromolecules* **1989**, *22*, 2224.
(23) Weiss, R. A.; Fitzgerald, J. J.; Kim, D. *Macromolecules* **1991**, *24*, 1071.
(24) Fan, X. D.; Bazuin, C. G. *Macromolecules* **1993**, *26*, 2508.
(25) Kim, J.-S.; Roberts, S. B.; Eisenberg, A.; Moore, R. B. *Macromolecules* **1993**, *26*, 5256.
(26) Hara, M.; Sauer, J. A. *J. Macromol. Sci., Rev Macromol. Chem. Phys.* **1994**, *C34* (3), 325.
(27) Avrami, M. J. *J. Chem. Phys.* **1939**, *7*, 1103.
(28) Hoffman, J. D.; Weeks, J. J. *J. Res. Natl. Bur. Stand., Part A* **1962**, *66*, 13.
(29) Cimmino, S.; Di Pace, E.; Martuscelli, E.; Silvestre, C. *Polymer* **1991**, *32*, 1080.
(30) Gianotti, G.; Valvassori, A. *Polymer* **1990**, *31*, 473.
(31) Arnauts, J.; Berghmans, H. *Polym. Commun.* **1990**, *31*, 343.
(32) Gvozdic, N. V.; Meier, D. J. *Polym. Commun.* **1991**, *32*, 493.
(33) Flory, P. J. *Principles of Polymer Chemistry*; Cornell University Press: Ithaca, NY, 1953.
(34) Pasztor, A. J., Jr.; Landes, B. G.; Karjala, P. J. *Thermochim. Acta* **1991**, 187.
(35) Su, Z.; Li, X.; Hsu, S. L. *Macromolecules* **1994**, *27*, 287.
(36) Otocka, E. P.; Kwei, T. K. *Macromolecules* **1968**, *1*, 401.
(37) Hara, M.; Jar, P.; Sauer, J. A. *Polymer* **1991**, *32*, 1622.
(38) Moelwyn-Hughes, E. A. *Physical Chemistry*, 2nd ed.; Pergamon Press: New York, 1961.
(39) Pauling, L. *Proc. R. Soc. London* **1927**, *A114*, 181.
(40) Hara, M.; Eisenberg, A.; Storey, R. F.; Kennedy, J. P. In *Coulombic Interactions in Macromolecular Systems*; Eisenberg, A., Bailey, F. E., Eds.; ACS Symposium Series 302; American Chemical Society: Washington, DC, 1986; Chapter 14.
(41) Leibler, L.; Rubinstein, M.; Colby, R. H. *Macromolecules* **1991**, *24*, 4701.
(42) Tsujita, Y.; Shibayama, K.; Takizawa, A.; Kinoshita, T. *J. Appl. Polym. Sci.* **1987**, *33*, 1307.
(43) Vanhoorne, P.; Jerome, R.; Teyssie, P.; Laupretre, F. *Macromolecules* **1994**, *27*, 2548.
(44) Horrin, J.; Jerome, R.; Teyssie, Ph.; Marco, C.; Williams, C. E. *Polymer* **1988**, *29*, 1203.

MA960003P